IJESRT
INTERNATIONAL JOURNAL OF ENGINEERING SCIENCES & RESEARCH TECHNOLOGY

PROBING INITIAL AND FINAL-STATE DISTRIBUTIONS FOR Pb+Pb COLLISIONS AT 2.76 TeV: TSALLIS-BOLTZMANN VS. q-WEIBULL FORMALISM

Bhaskar De
Department of Physics, Taki Government College, Taki-743429, West Bengal, India

DOI: 10.5281/zenodo.1242995

ABSTRACT
Transverse momentum spectra and Nuclear modification factors for production of various secondaries in different central Pb+Pb collisions at $\sqrt{s_{NN}}$ = 2.76 TeV have been analysed in the light of two generalized distributions --- Tsallis-Boltzmann and q-Weibull formalism --- to extract insights on the final stage as well as the initial stage of the fireball to understand the evolution process. Besides, the dependence of different parameters, involved in both the approaches, on centralities and mass of the secondaries, have also been discussed, in detail.
KEYWORDS: Relativistic Heavy Ion Collision, Inclusive Cross Section.

I. INTRODUCTION
The probing agents of the QGP medium produced in ultra-high energy nuclear reactions are the partons which are produced immediate after the initial hard scatterings and, hence, witness the evolution of the QCD medium. As this evolution process leaves it's traits on these initial-state partons through it's interaction with these partons, the final-state distribution is expected to be quite different from it's initial version. So, to understand the thermalization route completely it is required to extract knowledge on the nature and fluctuations of the initial-state as well as the final-state distribution simultaneously.

The initial stages suffer from intrinsic fluctuations due to formation of Color Glass Condensate, fluctuations in temperature and fluctuations in energy density and, hence, the initial system can be treated to be in a non-equilibrated state [1]. These microscopic memories can be present even in the distribution of the final-state hadrons. Besides, these initial-state partons experience further interactions with the expanding QCD medium in terms of elastic collision and medium induced gluon radiation [2-5] before final fragmentation into hadrons. Hence, the final-state is also to be expected away from its equilibrium. So, to extract information from initial-state as well as the final-state distributions one needs generalized statistics which are competent to describe the systems which are yet to reach equilibrium.

The generalized form of Boltzmann-Gibbs(BG) statistics within the framework of non-equilibrium statistics, as proposed by Tsallis [6-8] and being called Tsallis non-extensive statistics, has been proven, over the years, to be a good tool to analyse various particle yields to understand the thermo-dynamical evolution of the systems having long-range microscopic memories, long range correlations, self-similarity etc., [9-35]. On the other hand, another empirical statistical model, called Weibull model [36], capable of explaining the processes having fragmentation and sequential branching, is also being applied to analyse particle production at different high energy interactions [37-40]. To bring in the systems, which are yet to reach equilibrium, under the umbrella of Weibull model, a proposition of generalisation of this model, like generalised BG statistics, in the framework of Tsallis non-equilibrium q-statistics has already been made, and the utility of the modified version, namely q-Weibull model, in describing the particle yields has also been checked in few cases [1, 41-44].

In the present work, our aim is to study the initial-state and final-state distributions simultaneously, in a systematic way, through the change in parameter-values of a particular distribution function. To do so, our theoretical probing tool will be Tsallis-Boltzmann(TB) distribution and q-Weibull(qW) distribution. Though, the experimental data on final-state yields are available, the initial-state distributions cannot be measured experimentally. We will follow the formalism adopted in Ref. [35] to extract information, indirectly, on initial-

ISSN: 2277-9655
Impact Factor: 5.164
CODEN: IJESS7

state distributions through nuclear modifcation factor(R_{AA}). We will analyse, here, in the present study, the data on p_T-spectra and nuclear modification factor(R_{AA}) for different identified hadrons produced in different central Pb + Pb collisions at LHC energy $\sqrt{s_{NN}}$ = 2.76 TeV in the mid-rapidity interval to extract information on final-state distributions and initial-state distributions respectively.

The organization of the present work is as follows: a brief outline of the theoretical approach, to be used in the present study, has been presented in next section. The obtained results and a detailed discussion on it have been provided in Section 3. And the last section is preserved for the summary.

II. OUTLINE OF THE THEORETICAL APPROACH

We follow the formalism given in Ref. [28] to obtain the expressions for invariant yield of the particles on the basis of Tsallis-Boltzmann(TB) and q-Weibull distributions.

The Tsallis-Boltzmann distribution(neglecting the chemical potential) is given by,

$$n_i(E_i) = \left[1 + (q-1)\frac{E_i}{T}\right]^{\frac{1}{1-q}} \quad (1)$$

where n_i is the number of states available for energy E_i, T is the temperature and q is the non-extensive index. As $q \to 1$ the above equation returns to the usual Boltzmann distribution $e^{-\frac{E_i}{T}}$.

The same for q-Weibull distribution is given by [41]

$$\begin{aligned} n_i(E_i) &= p_0 \frac{k}{\lambda}\frac{E_i^{k-1}}{\lambda}\left[1 + (q-1)\frac{E_i^k}{\lambda}\right]^{\frac{1}{1-q}} \\ &= p_0' \frac{E_i^{k-1}}{\lambda}\left[1 + (q-1)\frac{E_i^k}{\lambda}\right]^{\frac{1}{1-q}} \end{aligned} \quad (2)$$

where p_0 is a proportionality constant, λ is a scale factor, k is the shape factor, $p_0' = p_0\frac{k}{\lambda}$ and q is the non-extensive parameter which determines the degree of deviation of the system from it's equilibrium. The scale factor, λ is directly proportional to the mean of the random variable [40]. So, in the present case, it is directly linked with the mean energy, or with the mean transverse momentum if the variable is transverse momentum p_T. For, $k = 1$ and $q \neq 1$, the above relation reduces to Tsallis-Boltzmann distribution and for $k = 1$ and $q = 1$ it gives back the usual Boltzmann distribution. It is quite clear that since $\lambda_{qW} = T_{TB}$ for $k = 1$ as q-Weibull distribution reproduces Tsallis-Boltzmann distribution for that value of k, the parameter λ can be treated as a temperature-like parameter for q-Weibull distribution and the Tsallis Temperature T can be treated to be directly linked with mean transverse momentum.

To keep the thermodynamic consistency one needs the constraints [28]

$$n_i^q = N \quad (3)$$

where N is the total number of particles. In the large volume limit we have,

$$\Sigma_i \to V\int\frac{d^3p}{(2\pi)^3} \quad (4)$$

Hence, total number of particles, for Tsallis-Boltzmann distribution, is given by,

$$N = gV\int\frac{d^3p}{(2\pi)^3}\left[1 + (q-1)\frac{E}{T}\right]^{\frac{q}{1-q}} \quad (5)$$

and that for q-Weibull distribution is given by,

$$\begin{aligned} N &= gV\int\frac{d^3p}{(2\pi)^3}(p_0')^q\left(\frac{E_i^{(k-1)}}{\lambda}\right)^q\left[1 + (q-1)\frac{E_i^k}{\lambda}\right]^{\frac{q}{1-q}} \\ &= gV\int\frac{d^3p}{(2\pi)^3}p\left(\frac{E_i^{(k-1)}}{\lambda}\right)^q\left[1 + (q-1)\frac{E_i^k}{\lambda}\right]^{\frac{q}{1-q}} \end{aligned} \quad (6)$$

where g is the degeneracy factor, V is the volume of the system and $p = (p'_0)^q$.
Hence, the invariant momentum distribution will take the form for Tsallis-Boltzmann distribution,

$$E\frac{d^3N}{dp^3} = \frac{gV}{(2\pi)^3}E\left[1+(q-1)\frac{E}{T}\right]^{\frac{q}{1-q}} \tag{7}$$

The energy, E, of the particle is given by

$$E = m_T\, coshy \tag{8}$$

where $m_T = \sqrt{m_0^2 + p_T^2}$ is the transverse mass and y is the rapidity.
So, the last expression for invariant yield will take the form

$$\frac{dN}{p_T\, dp_T\, dy} = \frac{gV}{(2\pi)^2}m_T\, coshy\left[1+(q-1)\frac{m_T\, coshy}{T}\right]^{\frac{q}{1-q}} \tag{9}$$

In the central rapidity it will be,

$$\frac{dN}{dp_T\, dy}|_{y=0}^{TB} = \frac{gV}{(2\pi)^2}\, p_T m_T\left[1+(q-1)\frac{m_T}{T}\right]^{\frac{q}{1-q}} \tag{10}$$

Similarly, this expression for q-Weibull distribution will be of the form

$$\frac{dN}{dp_T\, dy}|_{y=0}^{qW} = \frac{gV}{(2\pi)^2}\, p\, p_T m_T\left(\frac{m_T^{k-1}}{\lambda}\right)^q\left[1+(q-1)\frac{m_T^k}{\lambda}\right]^{\frac{q}{1-q}} = Cp_T m_T\left(\frac{m_T^{k-1}}{\lambda}\right)^q\left[1+(q-1)\frac{m_T^k}{\lambda}\right]^{\frac{q}{1-q}} \tag{11}$$

with $C = \frac{gV}{(2\pi)^2}\, p$ being a constant.

A point is to be noted here that $q \leq 1.22$ Tsallis-Boltzmann distribution[9], whereas, following the same argument, it can be shown that $q \leq \frac{k}{4} + 1$ for q-Weibull distribution.

Now, to extract information on the initial states, we follow the formalism adopted by Ref. [35]. It is assumed that the initial-state constituents undergo Brownian motions due to their interactions with the medium, and these motion can be described by Boltzmann transport equation,

$$\frac{df(x,p,t)}{dt} = \frac{\partial f}{\partial t} + \mathbf{v}.\nabla_x f + \mathbf{F}.\nabla_p f = C[f] \tag{12}$$

where $f(x,p,t)$ is the particle-distribution, **v** is the velocity, **F** is the external force and $C[f]$is the collision term for interaction between the particles and the medium. For a homogeneous medium($\nabla_x f = 0$), in absence of any external force(F = 0) and in the relaxation time picture, the above equation simplifies to

$$\frac{df(x,p,t)}{dt} = \frac{\partial f}{\partial t} = C[f] = -\frac{f - f_{eq}}{\tau} \tag{13}$$

where, f_{eq} is local Boltzmann equilibrium distribution and τ is the relaxation time for a non-equilibrium system to reach equilibrium.
The solution of the above equation along with the initial conditions, i.e. at $t = 0$, $f = f_{in}$ (distribution at the initial state) and at $t = t_f$, $f = f_{fin}$ (distribution at the final state), is given by,

$$f_{fin} = f_{eq} + (f_{in} - f_{eq})e^{-\frac{t_f}{\tau}} \tag{14}$$

where t_f is the freeze-out time.
Hence, the nuclear modi_cation factor takes the form [35],

$$R_{AA} = \frac{f_{fin}}{f_{in}} = \frac{f_{eq}}{f_{in}} + (1 - \frac{f_{eq}}{f_{in}})e^{-\frac{t_f}{\tau}} \tag{15}$$

The distribution for f_{eq} is given by the usual Boltzmann distribution, in the central rapidity region($y = 0$),

$$f_{eq} = \frac{gV}{(2\pi)^2}p_T m_T e^{-\frac{m_T}{T_{eq}}} \tag{16}$$

Hence, the final forms of the nuclear modification factor, R_{AA}, on the basis of eqn.(10) and eqn.(11), are given, respectively, by

$$R_{AA}|^{TB} = \frac{e^{-\frac{m_T}{T_{eq}}}}{\left[1+(q-1)\frac{m_T}{T}\right]^{\frac{q}{1-q}}} + (1 - \frac{e^{-\frac{m_T}{T_{eq}}}}{\left[1+(q-1)\frac{m_T}{T}\right]^{\frac{q}{1-q}}})e^{-\frac{t_f}{\tau}} \tag{17}$$

and

$$R_{AA}|^{qW} = \frac{e^{-\frac{m_T}{T_{eq}}}}{p\left(\frac{m_T^{k-1}}{\lambda}\right)^q\left[1+(q-1)\frac{m_T^k}{\lambda}\right]^{\frac{q}{1-q}}} + (1 - \frac{e^{-\frac{m_T}{T_{eq}}}}{p\left(\frac{m_T^{k-1}}{\lambda}\right)^q\left[1+(q-1)\frac{m_T^k}{\lambda}\right]^{\frac{q}{1-q}}})e^{-\frac{t_f}{\tau}} \tag{18}$$

III. RESULTS AND DISCUSSION

Table 1: Values of fitted parameters for Tsallis-Boltzmann Model with respect to the experimental data on transverse momentum spectra for different identified hadrons produced in Pb + Pb collision at 2.76 TeV

Range of Fits	centrality	T (GeV)	q	Reduced chi-square
π^0 $p_T \leq 6.0$ GeV/c	0-5%	0.13 ± 0.02	1.101 ± 0.002	1.529
	5-10%	0.14 ± 0.02	1.100 ± 0.007	1.162
	10-20%	0.13 ± 0.01	1.110 ± 0.006	1.816
	20-40%	0.112 ± 0.009	1.118 ± 0.005	1.971
	40-60%	0.106 ± 0.007	1.127 ± 0.004	0.951
	60-80%	0.101 ± 0.008	1.134 ± 0.008	0.599
$\pi^{\pm}$ $p_T \leq 6.0$ GeV/c	0-5%	0.113 ± 0.003	1.115 ± 0.002	1.582
	5-10%	0.112 ± 0.003	1.117 ± 0.002	1.216
	10-20%	0.108 ± 0.003	1.122 ± 0.002	1.741
	20-40%	0.102 ± 0.002	1.130 ± 0.002	1.464
	40-60%	0.090 ± 0.002	1.141 ± 0.002	1.038
	60-80%	0.082 ± 0.002	1.149 ± 0.002	0.178
$K^{\pm}$ $p_T \leq 6.0$ GeV/c	0-5%	0.216 ± 0.005	1.063 ± 0.003	1.823
	5-10%	0.210 ± 0.005	1.068 ± 0.003	1.775
	10-20%	0.199 ± 0.005	1.079 ± 0.003	1.578
	20-40%	0.182 ± 0.004	1.090 ± 0.002	1.290
	40-60%	0.144 ± 0.004	1.113 ± 0.002	1.337
	60-80%	0.123 ± 0.002	1.127 ± 0.001	1.261
$p/\bar{p}$ $p_T \leq 6.0$ GeV/c	0-5%	0.337 ± 0.004	1.031 ± 0.003	1.841
	5-10%	0.335 ± 0.004	1.031 ± 0.003	1.724
	10-20%	0.311 ± 0.004	1.041 ± 0.003	1.703
	20-40%	0.276 ± 0.003	1.055 ± 0.003	1.686
	40-60%	0.230 ± 0.002	1.069 ± 0.002	1.579
	60-80%	0.190 ± 0.001	1.080 ± 0.001	1.398
D^0 $p_T \leq 6.0$ GeV/c	0-10%	0.41 ± 0.03	1.09 ± 0.02	1.621
	30-50%	0.30 ± 0.02	1.13 ± 0.01	1.188

The equilibrium temperature, T_{eq}, has been kept at 160 MeV, throughout our analysis, to keep parity with Ref. [35]. Besides, the fits, obtained on the basis of Tsallis-Boltzmann distributions, are depicted with solid lines while those for q-Weibull are represented by dashed lines in all the figures.

Figure 1 represents the fits for transverse momentum spectra, obtained on the basis of both the distributions while Figure 2 to Figure 6 represent the fits for R_{AA}. The values of the different parameters obtained by the fits are tabulated in Table 1 to Table 5. Besides, the parameter values, we have also mentioned the p_T -range for which the good fits were obtained. It is observed from the tables and the Figure 1 to Figure 6 that Tsallis-Boltzmann distribution provides good fits for p_T-spectra in the range $p_T \leq 6$ GeV/c for all the secondaries while q-Weibull caters relatively wider range of data --- upto 20 GeV/c for pions and upto 16 GeV/c for heavier varieties like K-mesons, protons/antiprotons and D-mesons for most of the centralities.

But, the scenario gets changed, when we move to R_{AA} as far as TB is concerned. The fits in this case remain confined mainly in the range $1.4 \leq p_T \leq 12$ GeV/c for pions and kaons, and in the range $3 \leq p_T \leq 12$ for protons/antiprotons. This behaviour is in accordance with the findings reported in Ref. [35]. On the other hand, the qW distribution, once again, reproduces a wider range of data even in the low-p_T region compared to TB distributions. However, the lower range gets gradually shifted towards intermediate p_T for heavier secondaries. Data for D^0 production is available only for p_T> 1 GeV/c; and both the formalisms provide moderate fits (Figure 6) without exhibiting any noticeable difference. At the early stage of the evolution of the fireball, a bound state of heavy quarks called quarkonium($Q\bar{Q}$) can be formed. However in the presence of QGP the two color charges of this bound state gets screened from each other, which weakens the binding of this $Q\bar{Q}$ pair [45-48].The characteristic length of this screening is inversely proportional to the temperature of the medium.

This sequential dissociation may lead to suppressed production of bound quarkonium in the presence of QGP medium. Subsequently, these heavy quarks may hadronize by combining with light quarks. Since, the heavy

Table 2: Values of fitted parameters for q-Weibull Model with respect to the experimental data on transverse momentum spectra for different identified hadrons produced in Pb+Pb collision at $\sqrt{s_{NN}}$ = 2.76 TeV

Range of Fits	centrality	k	λ (GeV/c)	q	reduced chi-square
π^0 $p_T \leq 12.0$ GeV/c	0-5%	1.90 ± 0.03	0.27 ± 0.04	1.28 ± 0.03	1.719
	5-10%	1.78 ± 0.02	0.27 ± 0.02	1.26 ± 0.05	1.831
	10-20%	1.72 ± 0.01	0.23 ± 0.03	1.26 ± 0.03	1.498
	20-40%	1.52 ± 0.02	0.20 ± 0.01	1.23 ± 0.02	1.511
	40-60%	1.26 ± 0.02	0.15 ± 0.01	1.19 ± 0.01	1.326
	60-80%	1.04 ± 0.01	0.092 ± 0.003	1.151 ± 0.002	0.815
$\pi^\pm$ $p_T \leq 20.0$ GeV/c	0-5%	1.78 ± 0.06	0.27 ± 0.01	1.28 ± 0.02	1.388
	5-10%	1.69 ± 0.06	0.26 ± 0.03	1.26 ± 0.02	1.023
	10-20%	1.58 ± 0.05	0.23 ± 0.03	1.25 ± 0.01	0.975
	20-40%	1.37 ± 0.03	0.18 ± 0.02	1.21 ± 0.01	0.731
	40-60%	1.14 ± 0.02	0.120 ± 0.003	1.172 ± 0.006	0.583
	60-80%	1.00 ± 0.01	0.085 ± 0.006	1.147 ± 0.004	0.743
$K^\pm$ $p_T \leq 16.0$ GeV/c	0-5%	1.98 ± 0.01	0.45 ± 0.02	1.29 ± 0.02	1.744
	5-10%	1.98 ± 0.02	0.47 ± 0.02	1.30 ± 0.01	1.689
	10-20%	1.85 ± 0.02	0.42 ± 0.02	1.28 ± 0.02	1.565
	20-40%	1.66 ± 0.02	0.34 ± 0.01	1.253 ± 0.008	1.507
	40-60%	1.67 ± 0.03	0.32 ± 0.01	1.26 ± 0.02	1.333
	60-80%	1.67 ± 0.01	0.32 ± 0.02	1.26 ± 0.01	1.105
$p/\bar{p}$ $p_T \leq 16.0$ GeV/c	0-5%	1.68 ± 0.02	0.63 ± 0.01	1.18 ± 0.01	1.658
	5-10%	1.68 ± 0.02	0.63 ± 0.01	1.18 ± 0.01	1.539
	10-20%	1.64 ± 0.01	0.57 ± 0.02	1.18 ± 0.02	1.548
	20-40%	1.44 ± 0.03	0.41 ± 0.01	1.17 ± 0.01	1.721
	40-60%	1.53 ± 0.03	0.37 ± 0.01	1.20 ± 0.01	1.445
	60-80%	1.55 ± 0.03	0.34 ± 0.01	1.21 ± 0.01	1.255
D^0 $p_T \leq 16.0$ GeV/c	0-10%	1.02 ± 0.02	0.11 ± 0.01	1.16 ± 0.02	1.913
	30-50%	1.13 ± 0.03	0.10 ± 0.01	1.21 ± 0.03	1.038

quarks, generally, decay to quarks of different generations, these hadrons with heavy quarks can, ultimately, decay semileptonically to lighter hadrons in the low transverse momentum region [49]. Hence, these signatures of sequential dissociations might not be completely washed away in the final-state distributions in the low transverse momentum region. But, these effects were not incorporated in the formalism given in eqn.(12) for extracting information on initial-states from R_{AA}. So, this could be the reason for failing of the combination of eqn.(12) with Tsallis-Boltzmann distribution in catering low-p_T data for R_{AA}. But, the Weibull distribution is the genesis of the processes involving sequential fragmentation [37] and when it is combined with eqn.(12), the combination, given by eqn.(18), succeeded, to some extent, in catering the data on nuclear modifcation factor for low transverse momenta. However, the absence of eqn(12) or eqn.(15) in the final working formulae for extracting information on final-state distributions might be the cause to the success of both the theoretical distributions to cater the final-state spectra in the low-p_T region as both the formalisms are suitable for systems having fractal characters.

Both the distributions, when embedded in equation(12) through eqn.(15) for nuclear modification factor, exhibit a flat behaviour in the very high transverse momentum region, and, hence, the present formalism to extract information on initial-states along with the present distributions cannot be treated as competent enough to cater the data when there is a sharp rise in nuclear modification factor at very high-p_T as is evidenced in the cases of charged pions and kaons. In this region, the energy loss due to medium induced gluon radiation dominates the collisional energy loss by the partons formed immediate after the initial hard scatterings and travelling through the QGP medium. This effect was not incorporated, specifically, in the present form of Boltzmann transport equation(eqn.(12)) to deal with R_{AA}. The upper panels of the Figure 7 exhibit the nature of variation of the non-extensive parameter, q, obtained for Tsallis-Boltzmann distributions whereas the lower panels provide the same obtained for q-Weibull distributions. The values of q, obtained for initial states by both

ISSN: 2277-9655
Impact Factor: 5.164
CODEN: IJESS7

Table 3: Values of fitted parameters for Tsallis-Boltzmann Model with respect to the experimental data on nuclear modification factor for different identified hadrons produced in Pb+Pb collision at LHC

Range of Fits	centrality	T (GeV)	q	t_f/τ	reduced chi-square
π^0 $p_T \geq$ 1.4 GeV/c	0-5%	0.178 ± 0.002	1.002 ± 0.001	2.3 ± 0.1	0.430
	5-10%	0.176 ± 0.001	1.002 ± 0.001	1.98 ± 0.07	0.366
	10-20%	0.177 ± 0.001	1.003 ± 0.001	1.71 ± 0.06	0.478
	20-40%	0.174 ± 0.001	1.003 ± 0.001	1.43 ± 0.04	0.267
	40-60%	0.173 ± 0.002	1.004 ± 0.002	0.87 ± 0.04	0.287
	60-80%	0.174 ± 0.005	1.005 ± 0.002	0.50 ± 0.05	0.389
$\pi^\pm$ $12 \geq p_T \geq$ 1.4 GeV/c	0-5%	0.179 ± 0.002	1.002 ± 0.001	2.05 ± 0.05	0.495
	5-10%	0.179 ± 0.001	1.002 ± 0.002	1.87 ± 0.04	0.443
	10-20%	0.176 ± 0.001	1.003 ± 0.001	1.66 ± 0.03	0.338
	20-40%	0.176 ± 0.001	1.002 ± 0.001	1.30 ± 0.02	0.236
	40-60%	0.177 ± 0.002	1.004 ± 0.002	0.86 ± 0.03	0.087
	60-80%	0.182 ± 0.003	1.005 ± 0.002	0.52 ± 0.01	0.023
$K^\pm$ $12 \geq p_T \geq$ 1.4 GeV/c	0-5%	0.169 ± 0.001	1.004 ± 0.001	2.17 ± 0.06	0.448
	5-10%	0.168 ± 0.001	1.004 ± 0.001	1.97 ± 0.06	0.426
	10-20%	0.168 ± 0.002	1.004 ± 0.001	1.72 ± 0.05	0.358
	20-40%	0.167 ± 0.001	1.003 ± 0.001	1.34 ± 0.04	0.230
	40-60%	0.167 ± 0.001	1.004 ± 0.001	0.85 ± 0.02	0.064
	60-80%	0.173 ± 0.003	1.004 ± 0.001	0.47 ± 0.02	0.055
$p/\bar{p}$ $20 \geq p_T \geq$ 3 GeV/c	0-5%	0.155 ± 0.001	1.005 ± 0.001	1.69 ± 0.03	0.026
	5-10%	0.155 ± 0.001	1.005 ± 0.001	1.54 ± 0.02	0.012
	10-20%	0.153 ± 0.001	1.006 ± 0.002	1.28 ± 0.03	0.037
	20-40%	0.153 ± 0.001	1.006 ± 0.001	0.93 ± 0.02	0.029
	40-60%	0.151 ± 0.002	1.007 ± 0.002	0.53 ± 0.01	0.013
	60-80%	0.153 ± 0.001	1.007 ± 0.002	0.34 ± 0.03	0.046
D^0 $30 \geq p_T \geq$ 1 GeV/c	0-10%	0.149 ± 0.001	1.012 ± 0.004	1.73 ± 0.07	0.219
	30-50%	0.138 ± 0.002	1.020 ± 0.004	0.94 ± 0.06	0.162

Table 4: Values of fitted parameters for q-Weibull Model with respect to the experimental data on nuclear modification factor for neutral and charged pi-mesons produced in Pb+Pb collision

Range of Fits	centrality	k	λ (GeV/c)	q	t_f/τ	reduced chi-squre
π^0 $p_T \geq$ 0.7 GeV/c	0-5%	0.64 ± 0.01	0.021 ±0.002	1.002 ±0.001	2.16 ± 0.05	0.161
	5-10%	0.62 ± 0.01	0.016 ±0.002	1.002 ±0.001	1.88 ± 0.05	0.196
	10-20%	0.63 ± 0.02	0.020 ±0.003	1.002 ±0.001	1.64 ± 0.05	0.433
	20-40%	0.62 ± 0.01	0.018 ±0.002	1.003 ±0.001	1.32 ± 0.05	0.505
	40-60%	0.58 ± 0.01	0.012 ±0.002	1.003 ±0.001	0.82 ± 0.03	0.284
	60-80%	0.55 ± 0.02	0.010 ±0.004	1.005 ±0.001	0.50 ± 0.05	0.399
$\pi^\pm$ $12 \geq p_T$ $\geq$ 1 GeV/c	0-5%	0.67 ± 0.01	0.030 ±0.003	1.003 ±0.002	1.88 ± 0.02	0.431
	5-10%	0.68 ± 0.01	0.028 ±0.002	1.002 ±0.001	1.86 ± 0.02	0.196
	10-20%	0.67 ± 0.02	0.027 ±0.003	1.002 ±0.001	1.69 ± 0.02	0.234
	20-40%	0.69 ± 0.02	0.032 ±0.005	1.003 ±0.001	1.34 ± 0.02	0.288
	40-60%	0.64 ± 0.04	0.021 ±0.008	1.004 ±0.001	0.96 ± 0.02	0.322
	60-80%	0.60 ± 0.06	0.015 ±0.002	1.0043 ±0.0004	0.63 ± 0.02	0.199

the formalisms, have nearly same values[Fig.7(b) and Fig.7(d)] for a particular centrality despite the difference in fitting range for almost all the varieties. Above all, no significant dependence on centrality as well as on mass of the secondary is observed. As the parameter q is a measure of degree of fluctuations associated with the system, it can be assumed from these behavior that, at the initial stage, the degree of fluctuations is almost same for all the regions where the constituents of different secondaries emanates from and is independent of the

Table 5: Values of fitted parameters for q-Weibull Model with respect to the experimental data on R_{AA} for K-mesons, protons-antiprotons and D^0-mesons produced in Pb + Pb collision

Range of Fits	centrality	k	λ (GeV/c)	q	t_f/τ	reduced chi-square
$K^{\pm}$ $12 \geq p_T \geq$ 0.4 GeV/c	0-5%	0.67 ± 0.01	0.026 ±0.003	1.003 ±0.001	2.11 ± 0.04	0.411
	5-10%	0.66 ± 0.02	0.024 ±0.003	1.003 ±0.001	1.93 ± 0.04	0.394
	10-20%	0.66 ± 0.02	0.023 ±0.005	1.004 ±0.002	1.73 ± 0.05	0.147
	20-40%	0.66 ± 0.03	0.021 ±0.006	1.004 ±0.002	1.39 ± 0.05	0.580
	40-60%	0.59 ± 0.05	0.011 ±0.007	1.005 ±0.002	0.93 ± 0.04	0.377
	60-80%	0.60 ± 0.08	0.012 ±0.005	1.004 ±0.002	0.58 ± 0.02	0.205
$p/\bar{p}$ $20 \geq p_T \geq$ 1.2 GeV/c	0-5%	0.67 ± 0.02	0.018 ±0.003	1.004 ±0.001	1.70 ± 0.02	0.489
	5-10%	0.67 ± 0.02	0.017 ±0.003	1.004 ±0.002	1.56 ± 0.04	0.418
	10-20%	0.66 ± 0.02	0.015 ±0.004	1.005 ±0.002	1.27 ± 0.02	0.413
	20-40%	0.66 ± 0.03	0.014 ±0.006	1.006 ±0.001	0.97 ± 0.05	0.707
	40-60%	0.64 ± 0.05	0.012 ±0.007	1.006 ±0.002	0.55 ± 0.05	0.419
	60-80%	0.62 ± 0.05	0.011 ±0.005	1.007 ±0.002	0.42 ± 0.06	0.207
D^0 $30 \geq p_T \geq$ 1 GeV/c	0-10%	0.68 ± 0.01	0.012 ±0.001	1.016 ±0.006	1.74 ± 0.06	0.199
	30-50%	0.65 ± 0.01	0.007 ±0.001	1.018 ±0.006	0.98 ± 0.07	0.086

collisional geometry. Further, the initial systems are not far away from their equilibria as the magnitudes of q lie in the close vicinity of 1. Figure 7(a) and Figure 7(c) show the centrality dependence of the same parameter for final-state particles on the basis of Tsallis-Boltzmann and q-Weibull distributions respectively. There is a strong deviation in the values of q from its equilibrium value for both the cases. This increment in degree of fluctuations in the final-state distribution is the consequence of the interaction of the initial-state constituent partons with the expanding QCD medium. However, the centrality dependence of this particular parameter for Tsallis-Boltzmann distribution is in sharp contrast with those for q-Weibull distributions. As stated earlier, TB exhibits good performance for relatively low-$p_T$region compared to qW. And in this region, it is observed from Fig.7(a) that the system approaches equilibrium when one goes from peripheral to more central collisions. This behaviour of the system, on the basis of analysis of the low-p_T data, is in agreement with the hydrodynamic models of the evolution of the fireball where one expects emergence of low-$p_T$hadrons from a thermal system in local equilibrium due to presence of strong mass-dependent collective flow [50]. However, the incorporation of the data in higher-pT region changes the scenario. Here, for most of the varieties, q increases from peripheral to central collisions(Fig.7(c)). Here, more contributions are included from the particle-production mechanisms through pQCD hard scatterings of the high-$p_T$partons followed by fragmentation and hadronization and also from multigluon fluctuations [51]. These effect gradually increases from peripheral to central interactions and can be treated as the evidence for formation of a QCD medium in central Pb + Pb interactions. Besides, both the formalisms show that the massive particles are emanated from more equilibrated regions.

Plots in Figure 8 provide the nature of variation of Tsallis temperature T while those in Figure 9 give the variation of λ with respect to participant nucleons, N_{part}, for both final-states as well as initial-states. Once again, both of these parameters show approximately constant dependence on the collision-geometry for initial-states[Figure 8(b) and Figure 9(b)] as obtained from fitting R_{AA} data. This exhibition of independence of centrality of initial-state parameters indicates that the initial states are free from any nuclear-effect and might be formed at the surface of the nuclear medium. On the other hand. the centrality dependence of these parameters for the final-states is quite prominent. Both T_{TB} and T_{qW} exhibits increments in magnitude from their initial state-values and with respect to N_{part} from peripheral to central collisions. It has already been stated in the last section that both the parameters can be treated on the same footing. And it is an established fact that the average transverse momentum is positively correlated with particle density and energy density [52], and the local energy density is reflected in corresponding temperature. In relativistic heavy ion collisions energy is deposited, in the collisional region, by the participant nucleons. As the N_{part} increases with centrality, the energy density also increases. The initial partonic constituents after entering this dense QCD medium interact with it through several rescatterings which provide the initial partons more momentum-kicks. However, the high-p_T constituents lose energy through multi scatterings and gluon Bremsstrahlung(at very high-p_T) and populates the soft and intermediate- p_T region more. Hence, there is a rise in the average transverse momentum of the final-state distribution to the intermediate- p_T range alongwith rise in the corresponding local temperature, and these values

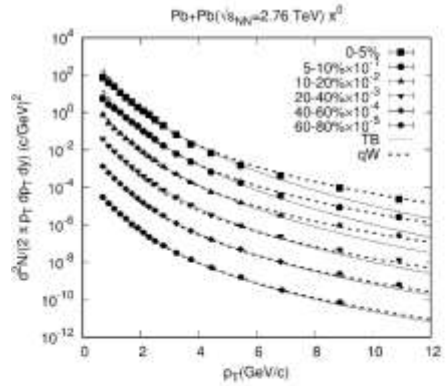

(a)

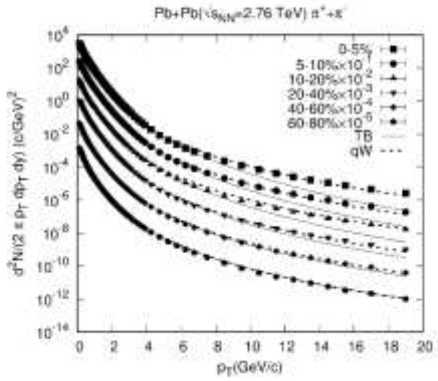

(b)

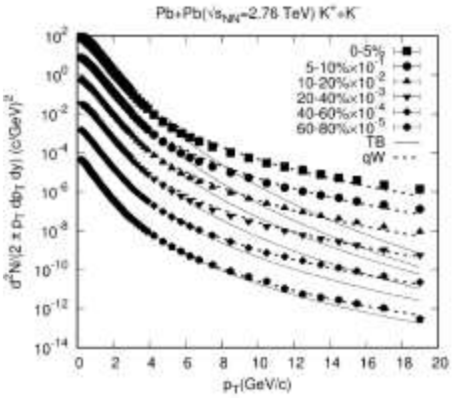

(c)

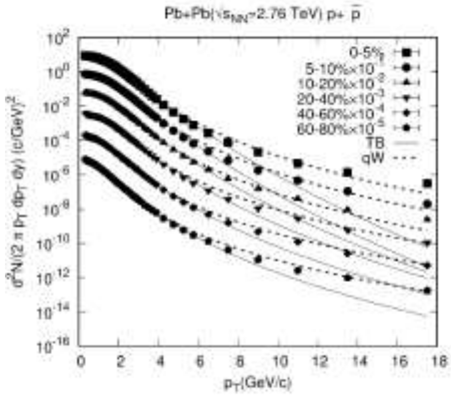

(d)

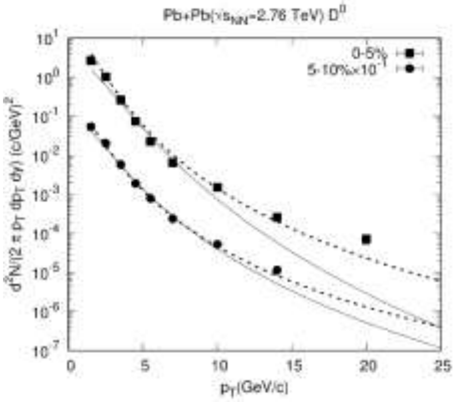

(e)

Figure 1: Plots of p_T-spectra for production of different identified hadrons in Pb + Pb interactions at 2.76 TeV. The fits for Tsallis-Boltzmann model(TB) are represented by solid lines while those for q-Weibull model(qW) are depicted by dashed lines. The experimental datapoints are derived from Ref. [55-57].

decrease from central to peripheral interactions due to decrement in collisional volume. Besides, the values of both the parameters, barring D^0-mesons, for initial states decrease with increasing mass of secondaries whereas those for final states exhibit completely opposite trend. This can be attributed to the fact that the heavier particles take relatively longer time to get thermalized.

For $k \neq 1$ and q > 1, the q-Weibull distribution gives a concave-upward curve. The curve with k > 1 falls more rapidly with respect to the curve with k < 1 for a fixed q and λ as p_T increases. Figure 10(a) shows the nature of this particular parameter for q-Weibull distribution for final-state particles whereas Figure 10(b) is for initial-state particles. It is observed that the values for initial state distribution lie in the range k < 1 for all the secondaries whereas those for final states fall in the range k > 1. This deviation clearly shows that the initial distribution just do not get scaled up with number of participant nucleons or number of binary collisions. Rather,

ISSN: 2277-9655
Impact Factor: 5.164
CODEN: IJESS7

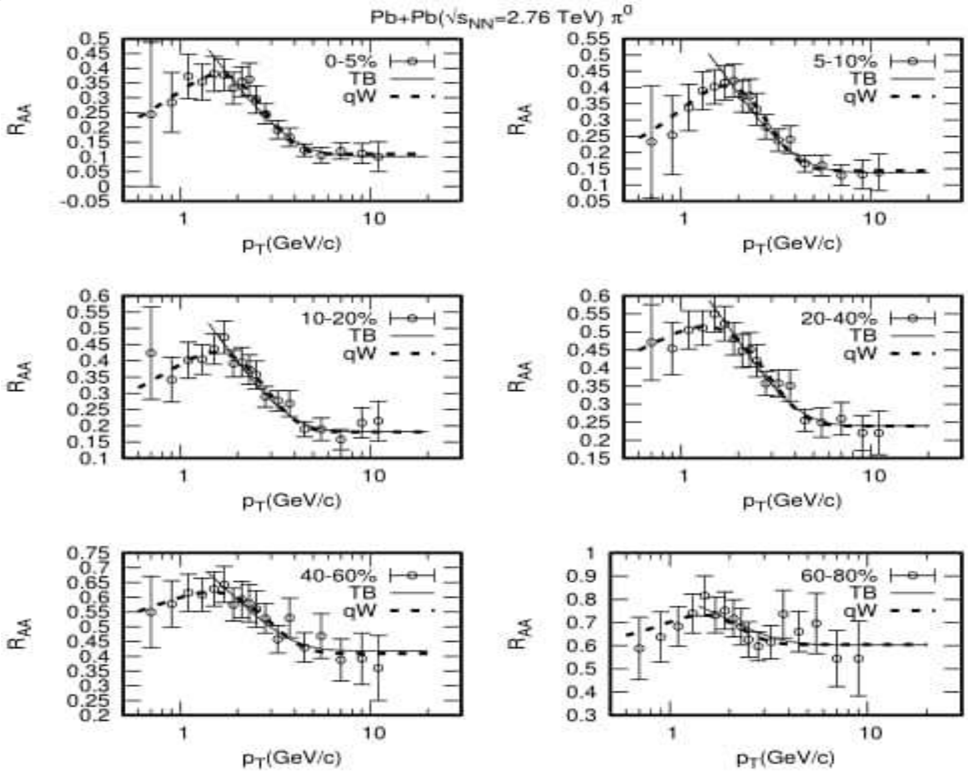

Figure 2: Plots of R_{AA} as the function of p_T for secondary neutral pi-mesons produced in different central Pb + Pb collisions at LHC energy 2.76 TeV. The solid lines are the fits for Tsallis-Boltzmann Model while the dashed ones for q-Weibull model(qW). The experimental data on $R_{AA}$are taken from Ref. [55].

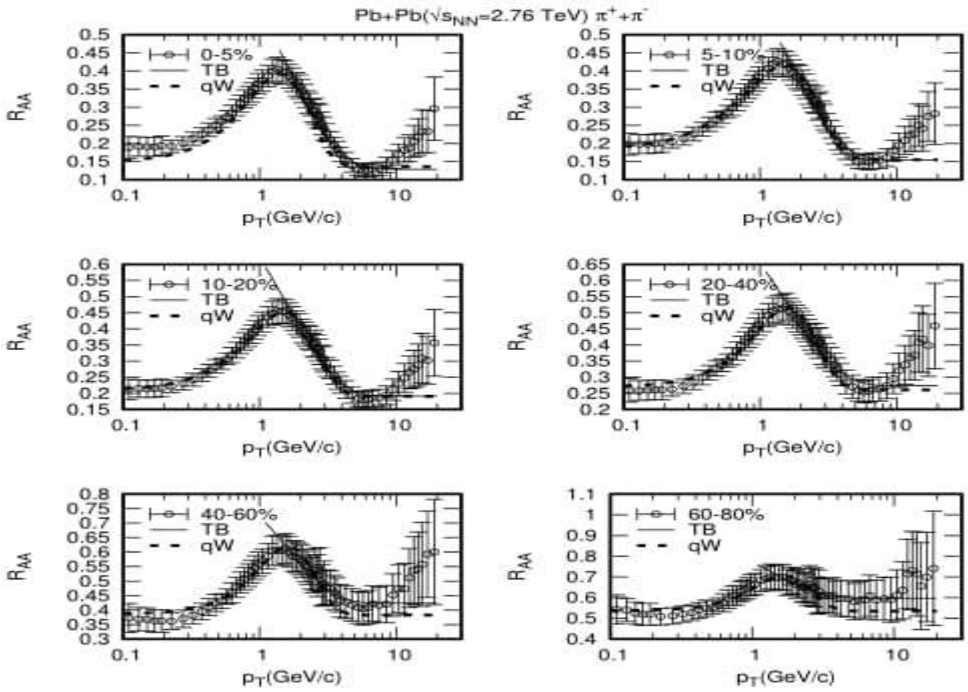

Figure 3: Plots of R_{AA} as the function of p_T for secondary charged pi-mesons produced in different central Pb + Pb collisions at LHC energy 2.76 TeV. The solid lines are the fits for Tsallis-Boltzmann Model while the dashed ones for q-Weibull model(qW). The experimental data on $R_{AA}$are taken from Ref. [56].

ISSN: 2277-9655
Impact Factor: 5.164
CODEN: IJESS7

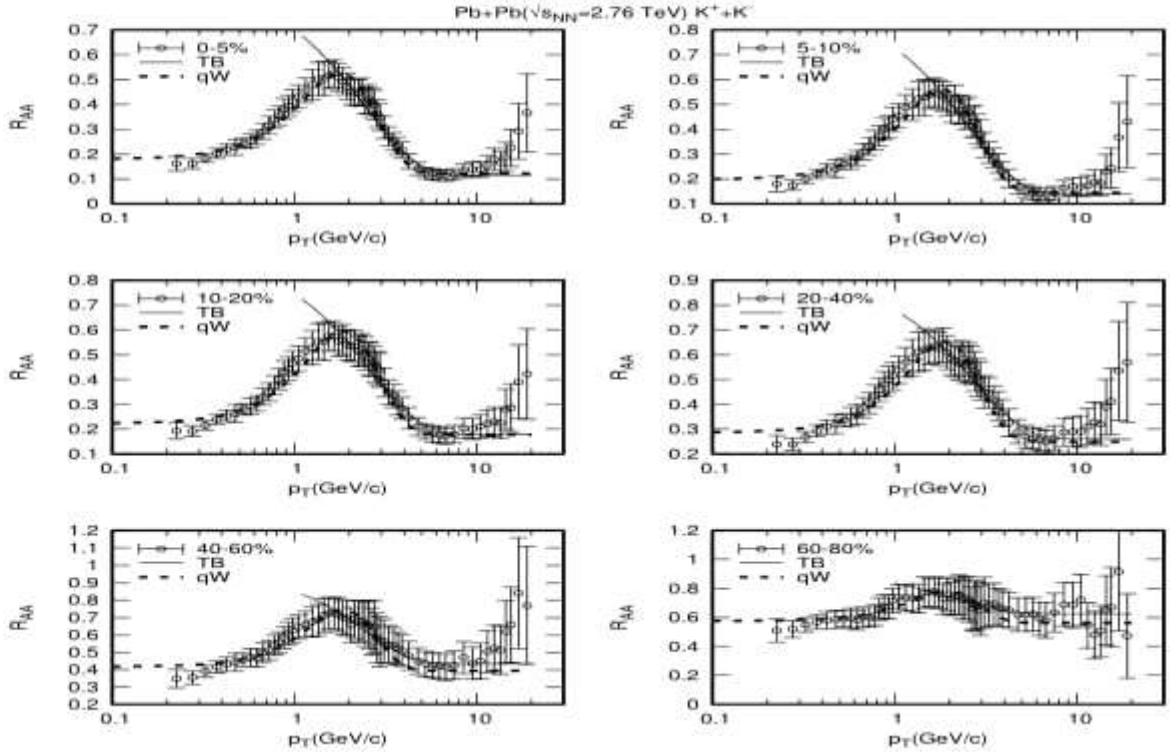

Figure 4: Plots of R_{AA} as the function of p_T for secondary charged K-mesons produced in different central Pb + Pb collisions at LHC energy 2.76 TeV. The solid lines are the fits for Tsallis-Boltzmann Model while the dashed ones for q-Weibull model(qW). The experimental data on $R_{AA}$are taken from Ref. [56].

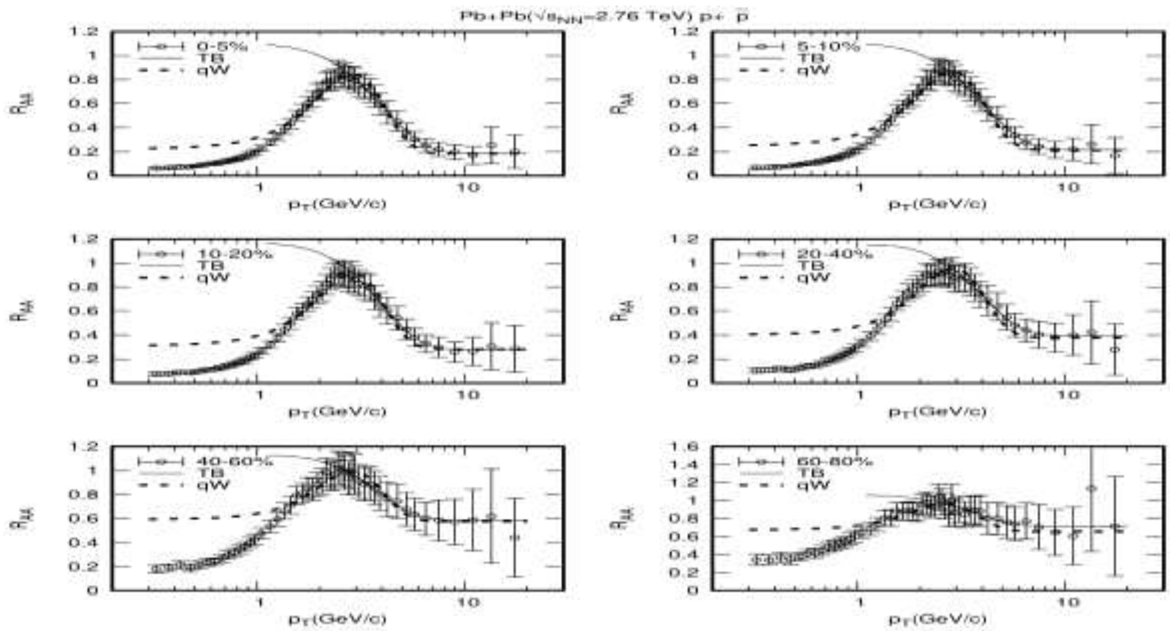

Figure 5: Plots of R_{AA} as the function of p_T for secondary protons/anti-protons produced in different central Pb + Pb collisions at LHC energy 2.76 TeV. The solid lines are the fits for Tsallis-Boltzmann Model while the dashed ones for q-Weibull model(qW). The experimental data on $R_{AA}$are taken from Ref. [56].

the final-state distribution exhibits a steep fall with increasing p_T compared to initial-ones due to increment in low-p_T multiplicity as the high-p_T partons lose energy through interaction with the QCD medium while travelling through the fireball formed in such ultrarelativistic heavy ion collisions. Besides, contributions from sequential dissociations of heavy quarkonia populates the lighter hadron-spectra in the low-p_T domain. As, this

ISSN: 2277-9655
Impact Factor: 5.164
CODEN: IJESS7

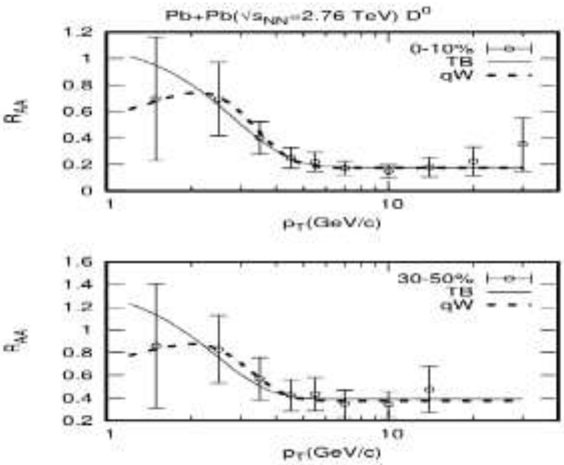

Figure 5: Plots of R_{AA} as the function of p_T for secondary D^0-mesons produced in different central Pb + Pb collisions at LHC energy 2.76 TeV. The solid lines are the fits for Tsallis-Boltzmann Model while the dashed ones for q-Weibull model(qW). The experimental data on $R_{AA}$are taken from Ref. [57].

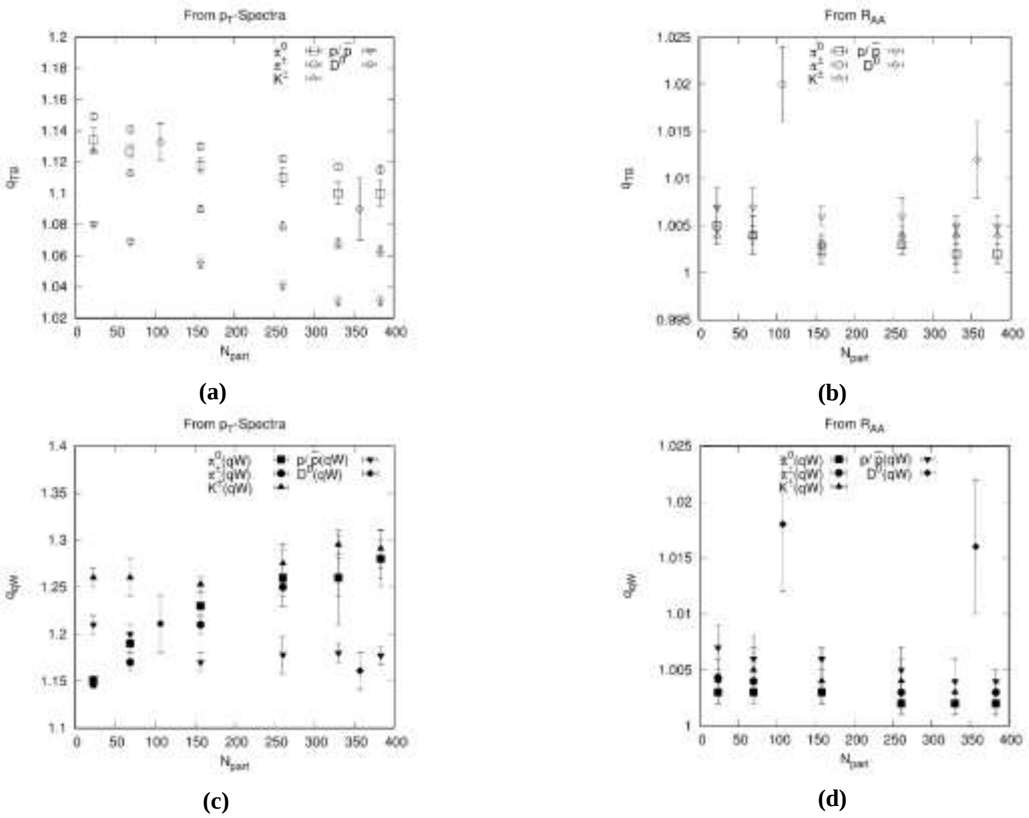

Figure 7: The nature of dependence of the non-extensive parameter, q, on the number of participant nucleons.

medium effect is more prominent in more central collisions, such deviation in k decreases from central to peripheral regions. Hence, the shape factor, k, is directly related with the dynamics of the particle production. Furthermore, D^0-meson consists of one of the heavier quarks, charm quark. And the energy loss by the medium-induced gluon radiation decreases with partonic mass [53]. This is reflected in the comparatively small deviation in k-values for D^0-mesons from initial states to final states. However, no concrete inference can be made, from the present analyses, as the data on D^0-mesons is not sufficient enough over the entire p_T -range compared to

ISSN: 2277-9655
Impact Factor: 5.164
CODEN: IJESS7

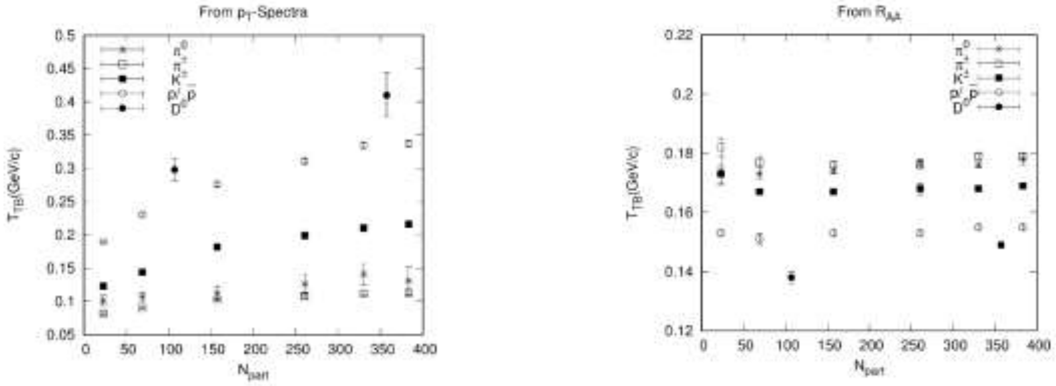

(a) **(b)**

Figure 8: Variation of Tsallis temperature as a function of number of participant nucleons.

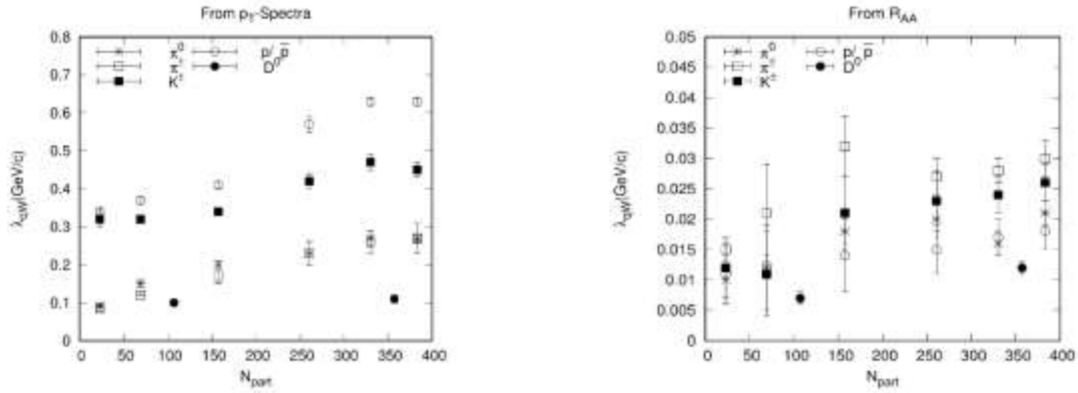

(a) **(b)**

Figure 9: Variations of λ with respect to number of participant nucleons.

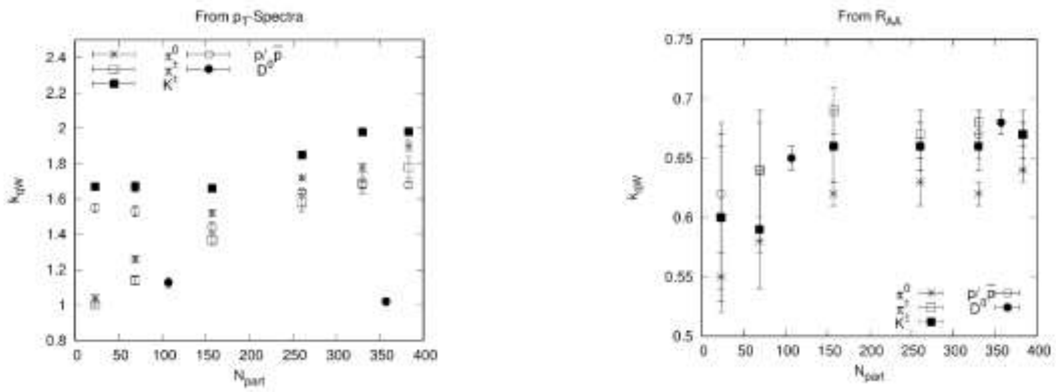

(a) **(b)**

Figure 10: Variations of k with respect to number of participant nucleons.

other varieties and the behaviours of the other parameters for D^0 mesons are always not quite explicable in the present context.

Figure 11 exhibits strong dependence of relative relaxation time, t_f/τ, on centrality. There is a sharp rise in relaxation time as one goes from central to peripheral interactions, which indicates at faster thermalization at central interactions. Furthermore, the magnitude of relaxation time for lighter hadrons is lesser than that for heavier ones, which, once again hints at relatively slower thermalization

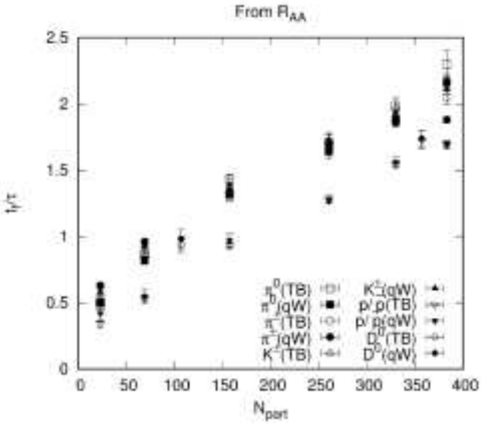

Figure 11: The nature of dependence of the relative relaxation time, t_f/τ, on the number of participant nucleons.

process for heavier secondaries. This observation is for both the formalisms and in agreement with the findings of Ref. [35].

IV. CONCLUSION

In the present study we have dealt with the invariant yield and nuclear modification factor for various secondary particles produced in mid-rapidity regions of central to peripheral Pb+Pb collisions at 2.76 TeV. Our theoretical tools for the current analysis were two generalized non-extensive distributions, namely, Tsallis-Boltzmann distribution and q-Weibull distribution. However, to analyse nuclear modification factor, these two distributions had to be embedded into another formalism based on Fokker-Planck equation where it was assumed that the partons, produced in initial hard scatterings, undergo Brownian motions due to collisional energy loss while travelling through the fireball produced in the ultra-high energy nuclear reactions without direct incorporation of the effect due to medium-induced gluon radiation or the effect due to color screening and subsequent dissociation of heavy quarks. This formalism to extract information from RAA fails to cater data at very high transverse momentum -region where gluon Bremsstrahlung plays dominant role, and, in some occasions, the low transverse momentum regions where fragmentation of heavy quarks due to Debye screening contributes. On the other hand, final-state transverse momentum spectra of the identified hadrons can be reproduced upto 6 GeV/c by Tsallis-Boltzmann distributions whereas upto 16 GeV by q-Weibull distributions for most of the secondaries. None of the distribution is capable of reproducing the data in the very high p_T -range which is in the purview of the perturbative QCD. The findings from the analyses of low and intermediate p_T -regions with Tsallis-Boltzmann distribution are in agreement with the hydrodynamical evolution picture of the fireball, whereas, the study of the wider p_T -range with q-Weibull distribution reveals more contributions from harder interactions between the initial partons with the fireball. In the latter case the medium influence gradually increases, in most of the cases, from peripheral to central collisions which indicates at the formation of a deconfined QCD medium in the Pb + Pb interactions at LHC energy. In a recent study [54], the contribution from the medium-induced gluon radiation was included in the original Langevin equation for Brownian motion to understand the evolution of the heavy quarks. Inclusion of such effects along with those from fragmentation of heavy quarkonia can make the present formalism competent to obtain more insights on the dynamical properties of the fireball in a unified manner.

REFERENCES

[1] S. Dash and D. P. Mahapatra, "Transverse Momentum Distribution in Heavy Ion Collision using q-Weibull Formalism", arXiv:1611.04025 and the references therein.
[2] D. d'Enterria, "Jet quenching", arXiv: nucl-ex/0902.2011.
[3] N. Armesto et. al., "Comparison of jet quenching formalisms for a quark-gluon plasma "brick"", Phys. Rev. C, vol. 86, pg 064904, 2012.
[4] G. Y. Qin, "Theory of jet quenching in ultra-relativistic nuclear collisions", Nucl. Phys. A vol. 931, pg 165, 2014
[5] J. Ghiglieri, G. D. Moore & D. Teaney, "Jet-medium interactions at NLO in a weakly-coupled quark-gluon plasma" , Jour. High. Ener. Phys., vol. 2016, pg 095, 2016.
[6] C. Tsallis, "Possible generalization of Boltzmann-Gibbs statistics", Jour. Stat. Phys., vol. 52, pg. 479, 1988.

[7] C. Tsallis: Lecture Notes on Physics - Nonextensive Statistical Mechanics and It's Applications 560/2001, 3 (Springer, 2001).
[8] C. Tsallis, "Nonadditive entropy: the concept and its use", Eur. Phys. Jour. A, vol. 40, pg. 257, 2009.
[9] C. Beck, "Nonextensive methods in turbulence and particle physics", Physica A, vol. 305, pg. 209, 2002.
[10] C. Beck, "Superstatistics in high-energy physics" Eur. Phys. Jour A, vol. 40, pg. 267, 2009.
[11] G. Wilk and Z. Wlodarczyk, "Interpretation of the Nonextensivity Parameter q in Some Applications of Tsallis Statistics and Lévy Distributions", Phys. Rev. Lett., vol. 84, pg. 2770, 2000.
[12] G. Wilk and Z. Wlodarczyk, "Power laws in elementary and heavy-ion collisionsA story of fluctuations and nonextensivity?" Eur. Phys. Jour. A, vol. 40, pg. 299, 2009.
[13] G. Wilk and Z. Wlodarczyk, "Equivalence of volume and temperature fluctuations in power-law ensembles", Jour. Phys. G, vol. 38, pg. 065101, 2011.
[14] T. S. Biro and G. Purcsel, "Nonextensive Boltzmann Equation and Hadronization", Phys. Rev. Lett, vol. 95, pg. 162302, 2005.
[15] T. S. Biro and E. Molnar, "Non-extensive statistics, relativistic kinetic theory and fluid dynamics" Eur. Phys. Jour. A, vol. 48, pg. 172, 2012.
[16] G. Biro, G. G. Barnafoldi, T. S. Biro and K. Urmossy, "Application of the Non-extensive Statistical Approach to High Energy Particle Collisions", AIP Conference Proceedings vol. 1853, pg. 080001, 2017
[17] M. Biyajima et al, "Analyses of k_T distributions at RHIC by means of some selected statistical and stochastic models", Eur. Phys. Jour. C, vol. 40, pg. 243, 2005.
[18] M. Biyajima et al, "Modified Hagedorn formula including temperature fluctuation: Estimation of temperatures at RHIC experiments", Eur. Phys. Jour. C, vol. 48, pg. 597, 2006.
[19] W. M. Alberico and A. Lavagno, "Non-extensive statistical effects in high-energy collisions", Eur. Phys. Jour. A, vol. 40, pg. 313, 2009.
[20] A. Lavagno, P. Quarati and A. M. Scarfone, "Nonextensive relativistic nuclear and subnuclear equation of state", Braz. Jour. Phys., vol. 39, pg. 457, 2009.
[21] G. Kaniadakis, "Relativistic Entropy and Related Boltzmann Kinetics", Eur. Phys. Jour. A, vol. 40, pg. 275, 2009.
[22] T. Kodama and T. Koide, "Dynamical origin of power spectra", Eur. Phys. Jour. A, vol. 40, pg.289, 2009.
[23] T. Wibig: "Constrains for non-standard statistical models of particle creations by identified hadron multiplicity results at LHC energies", Eur. Phys. Jour. C, vol. 74, pg. 2966, 2014.
[24] A. Deppman, "Properties of hadronic systems according to the nonextensive self-consistent thermodynamics", Jour. Phys. G, vol. 41, pg. 055108, 2014.
[25] L. Marques, E. Andrade-II and A. Deppman, "Nonextensivity of hadronic systems", Phys. Rev. D, vol. 87, pg 114022, 2013
[26] A. Deppman, "Thermodynamics with fractal structure, Tsallis statistics, and hadrons", Phys. Rev. D, vol. 93, pg. 054001, 2016.
[27] J. Cleymans and D. Worku, "Relativistic thermodynamics: Transverse momentum distributions in high-energy physics", Eur. Phys. Jour. A, vol. 48, pg. 160, 2012.
[28] J. Cleymans and D. Worku, "The Tsallis distribution in proton–proton collisions at $\sqrt{s}$= 0.9 TeV at the LHC", Jour. Phys. G, vol. 39, pg. 025006, 2012.
[29] T. Bhattacharyya et al, "Radial flow in non-extensive thermodynamics and study of particle spectra at LHC in the limit of small (q - 1)", Eur. Phys. Jour. A. vol. 52, pg. 30, 2016.
[30] H. R. Wei, F. H. Liu and R. A. Lacey et al, "Disentangling random thermal motion of particles and collective expansion of source from transverse momentum spectra in high energy collisions", Jour. Phys. G, vol. 43, pg. 125102, 2016
[31] H. R. Wei, F. H. Liu and R. A. Lacey et al, "Kinetic freeze-out temperature and flow velocity extracted from transverse momentum spectra of final-state light flavor particles produced in collisions at RHIC and LHC", Eur. Phys. Jour. A, vol. 52, pg. 102, 2016
[32] A. Parvan, "Comparison of Tsallis statistics with the Tsallis-factorized statistics in the ultrarelativistic pp collisions", Eur. Phys. Jour. A, vol. 52, pg. 355, 2016
[33] B. De, "Non-extensive statistics and a systematic study of meson-spectra at LHC energy $\sqrt{s_{NN}}$ = 2.76 TeV", Eur. Phys. Jour. A, vol. 50, pg. 70, 2014.

[34] B. De, "Non-extensive statistics and understanding particle production and kinetic freeze-out process from p_T-spectra at 2.76 TeV" Eur. Phys. Jour. A, vol. 50, 138, 2014.
[35] S. Tripathy et al, "Transverse-momentum spectra and nuclear modification factor using Boltzmann Transport Equation with flow in Pb+Pb collisions at $\sqrt{s_{NN}} = 2.76$ TeV", Eur. Phys. Jour. A, vol. 52, pg. 289, 2016.
[36] W. Weibull, "A Statistical Distribution Function of Wide Applicability", Jour. App. Mech., vol. 18, pg. 293, 1951.
[37] W. K. Brown and K. H. Wohletz, "Derivation of the Weibull distribution based on physical principles and its connection to the Rosin–Rammler and lognormal distributions", Jour. Appl. Phys. 78(1995) 2758.
[38] W. K. Brown, "A Theory of Sequential Fragmentation and Its Astronomical Applications ", Jour. Astr. Phys., vol. 10, pg. 89, 1989.
[39] S. Dash et al, "Weibull model of multiplicity distribution in hadron-hadron collisions", Phys. Rev. D, vol. 93, pg. 114022, 2016.
[40] S. Dash et al, "Multiplicity distributions in e^+e^- collisions using Weibull distribution", Phys. Rev. D, vol. 94, 074044, 2016.
[41] S. Picoli et al, "q-exponential, Weibull, and q-Weibull distributions: an empirical analysis", Physica, vol. 324, pg. 678, 2003.
[42] N. K. Behera et al, "Charged-particle multiplicity and transverse-energy distribution using the Weibull-Glauber approach in heavy-ion collisions", Phys. Rev. C, vol. 96, pg. 054906, 2017
[43] A. K. Pandey et al, "Weibull distribution and the multiplicity moments in pp(p$\bar{\text{p}}$) collisions", Phys. Rev. D , vol. 96, pg. 074006, 2017.
[44] C. Y.Wong: Introduction to High-Energy Heavy-Ion Collision, World Scientific Publishing Co., Singapore, pgs 344-354.
[45] T. Matsui & H. Satz, "J/Ψ Suppression by Quark-Gluon Plasma Formation", Phys. Lett. B, Vol. 178, pg. 416, 1986.
[46] S. Digal, P. Petreczky & H. Satz, "Quarkonium feed-down and sequential suppression", Phys. Rev. D vol. 64, pg. 094015, 2001.
[47] F. Karsch, D. Kharzeev & H. Satz, "Sequential charmonium dissociation", Phys. Lett. B, vol. 637, pg. 75, 2006.
[48] S. Chatrchyan et al (CMS Collaboration), "Observation of Sequential Y Suppression in PbPb Collisions", Phys. Rev. Lett., vol. 109, pg. 222301, 2012.
[49] J. D. Richman & P. R. Burchat, "Leptonic and semileptonic decays of charm and bottom hadrons", Rev. Mod. Phys., vol. 67, pg. 893, 1995.
[50] P. Kolb & U Heinz, "Hydrodynamic description of ultrarelativistic heavy-ion collisions", Quark Gluon Plasma 3, Edited by R.C. Hwa and X.-N. Wang, World Scientific, Singapore; arXiv:nucl-th/0305084.
[51] I. Vitev, "Testing the theory of QGP-induced energy loss at RHIC and the LHC", Phys. Lett. B, vol. 639, pg. 38, 2006.
[52] T. H. Burnett, "Average transverse momentum and energy density in high-energy nucleus-nucleus collisions" Phys. Rev. Lett., vol. 57, pg. 3249, 1986.
[53] P. Foka & M. A. Janik, "An overview of experimental results from ultra-relativistic heavy-ion collisions at the CERN LHC: hard probes", Rev. in Phys., vol. 1, pg. 172, 2016.
[54] S. Cao et al, "Collisional vs. Radiative Energy Loss of Heavy Quark in a Hot and Dense Nuclear Matter", Nucl. Phys. A, vol. 904-905, pg. 653c, 2013.
[55] The Alice Collaboration, "Neutral pion production at midrapidity in pp and Pb–Pb collisions at $\sqrt{s_{NN}} = 2.76$ TeV", Eur. Phys. Jour. C, vol. 74, pg. 3108, 2014.
[56] The Alice Collaboration(J. Adam et al.), "Centrality dependence of the nuclear modification factor of charged pions, kaons, and protons in Pb-Pb collisions at $\sqrt{s_{NN}} = 2.76$ TeV", Phys. Rev. C, vol. 93, pg. 034913, 2016.
[57] The Alice Collaboration, "Transverse momentum dependence of D-meson production in Pb-Pb collisions at $\sqrt{s_{NN}} = 2.76$ TeV", Jour. High Ener. Phys., vol. 03, pg. 081, 2016.

CITE AN ARTICLE

De, B. (2018). PROBING INITIAL AND FINAL-STATE DISTRIBUTIONS FOR Pb+Pb COLLISIONS AT 2.76 TeV: TSALLIS-BOLTZMANN VS. q-WEIBULL FORMALISM. *INTERNATIONAL JOURNAL OF ENGINEERING SCIENCES & RESEARCH TECHNOLOGY*, *7*(5), 218-232.